Wi-Diag : robust multi-subject abnormal gait diagnosis with commodity Wi-Fi

Lei Zhang, Yazhou Ma, Xiaojie Fan, Xiaochen Fan, Yonggang Zhang, Zhenxiang Chen, Xianyi Chen, Daqing Zhang

Wi-Diag:Robust Multi-subject Abnormal Gait Diagnosis with Commodity Wi-Fi

Lei Zhang, *Member, IEEE,* Yazhou Ma, Xiaojie Fan, Xiaochen Fan, *Member, IEEE,* Yonggang Zhang, *Member, IEEE,* Zhenxiang Chen, *Member, IEEE,* Xianyi Chen, *Member, IEEE,* and Daqing Zhang, *Fellow, IEEE*

***Abstract*—The existing commodity Wi-Fi based human gait recognition systems mainly focus on a single subject due to the challenges of multi-subject walking monitoring. To tackle the problem, we propose Wi-Diag, the first commodity Wi-Fi based multi-subject abnormal gait diagnosis system that leverages only one pair of off-the-shelf commercial Wi-Fi transceivers to separate each subject's gait information and maintains an excellent performance when the scenario changes. It is an intelligent multi-subject gait diagnosis system that can release an experienced doctor from heavy load work. Multi-subject abnormal gait diagnosis is modeled as a Blind Source Separation (BSS) issue, and multi-subject walking mixed signals are efficiently separated by Independent Component Analysis (ICA) approach. This fact is verified by comprehensive theoretical derivation and experimental validation. In addition, CycleGAN is leveraged to mitigate the environmental dependency so that Wi-Diag can be robust when the scenario changes. The excellent performance of Wi-Diag is verified by extensive experiments. The average mean diagnosis accuracy with a maximum group size of four and various scenarios is 87.77%.**

***Index Terms*—Channel State Information (CSI), Multi-subject Abnormal Gait Diagnosis, Blind Source Separation(BSS)**

This work is supported by the Natural Science Foundation of Tianjin under Grant No. 22JCYBJC00120, is partial funded by the European Union through the Horizon EIC pathfinder challenge project SUSTAIN (project number 101071179) and the Opening Fund of Shandong Provincial Key Laboratory Of Network based Intelligent Computing. (Lei Zhang and Yazhou Ma are co-first authors with equal contributions.) (Corresponding author: Daqing Zhang.)

Lei Zhang, Yazhou Ma, and Xiaojie Fan are with the College of Intelligence and Computing and the Tianjin Key Laboratory of Advanced Network Technology and Application, Tianjin University, Tianjin 300050, China. Lei Zhang is also with the State Key Laboratory for Novel Software Technology, Nanjing University, P.R. China, and with Shandong Provincial Key Laboratory of Network Based Intelligent Computing, University of Jinan, Jinan 250022, China. (e-mail: {lzhang, yazhouma, funfunfunny}@tju.edu.cn).

Xiaochen Fan is with the Institute for Electronics and Information Technology in Tianjin, Tianjin 300467, China, and with the Department of Electronic Engineering, Tsinghua University, Beijing 100084, China. (e-mail: fanxiaochen33@gmail.com).

Yonggang Zhang is with Key Laboratory of Symbolic Computation and Knowledge Engineer (Jilin University), Ministry of Education, Changchun 130012, China. (e-mail: zhangyg@jlu.edu.cn).

Zhenxiang Chen is with Shandong Provincial Key Laboratory of Network Based Intelligent Computing, University of Jinan, Jinan 250022, China, and with the school of information science and engineering, University of Jinan, Jinan 250022, China. (e-mail: zxchen@ujn.edu.cn).

Xianyi Chen is with Engineering Research Center of Digital Forensics, Ministry of Education, Nanjing University of Information Science and Technology, Nanjing 210044, China, and with the School of Computer and Software, Nanjing University of Information Science and Technology, Nanjing 210044, China. (e-mail: 002582@nuist.edu.cn).

Daqing Zhang is with the Télécom SudParis, IP Paris, France. (e-mail: daqing.zhang@telecom-sudparis.eu).

I. Introduction

WALKING is a very common movement in life. However, as people get older, their gaits begin to change, and walking states become unstable [1]. That is also known as gait disorder and is associated with falling complications. An abnormal gait is an irregular or abnormal walking pattern in humans. This abnormality may be caused by a variety of factors, such as neurological or musculoskeletal disorders, post-traumatic recovery, or post-surgery rehabilitation [2]. If this happens to a normal person, the gait abnormalities usually indicate brain function deterioration and a future risk of dementia, *e.g.,* Parkinson disease [3], [4], [5]. The types of abnormal gaits include spastic gait, scissors gait, steppage gait, waddling gait, propulsive gait, parkinsonian gait, and other abnormal gaits [6], [7]. Typically, normal gait is achieved through biomechanical mechanisms such as movement coordination, balance control, and gait rhythm. Thus, abnormal gait can be detected and diagnosed by analyzing the biomechanical features and movement patterns during walking.

Nowadays, with the improvement in living standards, everyone is more concerned about health issues. Every year, there will be a large number of people taking the special physical examination on gait inspection, especially brain disorder patients [8]. Meanwhile, the doctors can make a preliminary diagnosis based on the patient's gait. Early gait abnormalities detection and timely intervention are beneficial to disease treatment. However, when there are lots of people, gait testing one by one is a big amount of work for an experienced doctor. It is very necessary to build a convenient and smart gait diagnosis system which has the capability to detect abnormal gaits by group and release the doctors from intensive work.

Recently, the extensive deployment of Wi-Fi in indoor environments has enabled the analysis of human activities using Wi-Fi signals. The availability of CSI in Wi-Fi has substantially facilitated the progress of human activities sensing. And it has gained significant attention due to its noninvasive nature, ubiquity, better coverage, the fact that it requires little to no special hardware or modifications to existing hardware, and its ability to preserve privacy. These facts set it apart from other forms of gait recognition, such as camera-based methods [9], ambient floor sensor-based approaches [10], and wearable device-based techniques [11]. Wi-Fi based gait recognition has been extensively researched, with studies such as [12]–[16] highlighting its potential benefits.

Current research on commodity WiFi-based gait recognition primarily centered on the single-subject setting [12]–[16], neglecting the challenges presented by the multi-subject environment. In this context, the CSI dynamics are influenced by the motions of multiple subjects, making it challenging to derive the walking patterns of each individual accurately [17], [18]. In addition, the current gait monitoring research mainly works on gait recognition and there is hardly research on abnormal gait diagnosis. Moreover, the existing commercial Wi-Fi based gait recognition systems have better recognition accuracy in a single environment. The system performance will degrade when the test scenario changes [12]–[16], which is called environmental dependency.

There are two significant challenges. The first challenge is the separation of walking-induced signals of multiple subjects. This is crucial to distinguish abnormal gaits. In a multi-subject scenario, the additive effect [19], [20] negatively impacts the signals received at the Wi-Fi receiver. Furthermore, when multiple individuals walk simultaneously, different limbs move at varying speeds, causing the signals received to be a combination of reflections from various limbs. How to separate each subject's gait from the received mixed signals is a crucial challenge.

The other major challenge is that wireless signals received at the Wi-Fi receiver often contain important domain-specific information due to signal penetration, reflection, and diffraction from objects in the environment [21], [22]. Consequently, a gait recognition model trained on a particular domain may exhibit less optimal performance in other domains.

To address those issues above, the first commodity Wi-Fi based multi-subject abnormal gaits diagnosis system, Wi-Diag, is introduced. By utilizing a pair of off-the-shelf commodity Wi-Fi transceivers, Wi-Diag can achieve the multi-subject abnormal gait diagnosis in various scenarios and maintain excellent performance. The ability to utilize multiple antennas on commercial Wi-Fi transceivers is the crucial driver of Wi-Diag. A theoretical analysis of the multi-subject induced CSI dynamics proves that the reflected signals from multiple subjects are independent, non-Gaussian, and linearly combined on each receiving antenna. Therefore, the multi-subject abnormal gait diagnosis process is formulated for the famous Blind Source Separation (BSS) issue [23], and it seeks to separate source signal from multidimensional combined observation signal and remove noise. The assumptions are the number of participating subjects is known beforehand, and each subject walks along one predetermined straight path simultaneously.

In the Wi-Diag system, the CycleGAN is leveraged to achieve domain adaptation and mitigate environment dependency. Specifically, in the Wi-Diag system, by adopting the CycleGAN model, the gait information of one subject in one domain can be transformed into the same subject's gait information in the other domain while keeping the gait information consistent across various domains. The potential application of Wi-Diag is smart healthcare. For instance, in the medical examination center, Wi-Diag can provide early diagnosis and release the doctors from the intensive work by examining subjects' gaits by group and discovering the abnormal gaits.

In brief, our work's key contributions are outlined as follows:

- We achieve the Wi-Diag, a multi-subject abnormal gait diagnosis system that leverages two off-the-shelf Wi-Fi transceivers to achieve high accuracy, which involves framing the process as a Blind Source Separation issue. And to separate all subject's CSI dynamics from the combined signals at the receiver, the ICA technique is utilized.
- We apply the CycleGAN model to reduce the environmental dependence problem. The gait information of an individual in one environment can be transformed into their corresponding gait information in another, ensuring consistency across multiple domains.
- Wi-Diag is prototyped by utilizing only one pair of commodity Wi-Fi transceivers, and extensive experiments have evaluated it. Wi-Diag is the first wireless sensing system in that multi-subject's simultaneous walking gaits can be distinguished, and satisfied performance can be maintained even in changed scenarios. This represents a superior performance compared to existing methods.

To present our research in a clear and organized manner, the study is structured as follows: Sec.2 surveys currently proposed methods. Sec. 3 proposes a Wi-Fi-based multi-subject abnormal gait diagnosis system, Wi-Diag, which explains how the Independent Component Analysis (ICA) method separates each subject's gait information and how CycleGAN works for environment dependence mitigation. Sec.4 presents the prototyping of the Wi-Diag and the comprehensive experiments conducted. In Sec.5, the limitations of Wi-Diag are discussed. Finally, the paper concludes with Sec.6.

II. Related Work

A. Gait Recognition and Abnormal Gait Distinction

Human abnormal gait distinction and gait recognition is a significant application domain and has garnered considerable attention. Extensive sensing approaches have been explored in this field, including camera-based methods, [9], [24], ambient floor sensor-based approaches [10], [25], and wearable sensor-based techniques [11], [26]. However, there are limitations associated with all of these approaches. The vision-based methods for gait recognition are less desired due to the privacy violation and light sensitiveness [9], [24]. The ambient floor sensor-based gait recognition systems require to install the ambient environment sensors beforehand [10], [25]. In addition, distinguishing activity-induced data from environmental-related data can be challenging. Wearable sensor-based techniques [11], [26] utilize accelerometers, magnetometers and gyroscopes etc., integrated with smartphones and some wearable devices to collect data for further analysis, and it is inconvenient to carry the wearable sensors. So far, there have been considerable advancements in commercial wireless Wi-Fi based gait recognition technologies. In WiWho, identity authentication is implemented through the participants' gait information using WiFi CSI. Only one person can be authenticated at a time. In WifiU [14], spectrograms are utilized to obtain the gait patterns of an individual, and features are

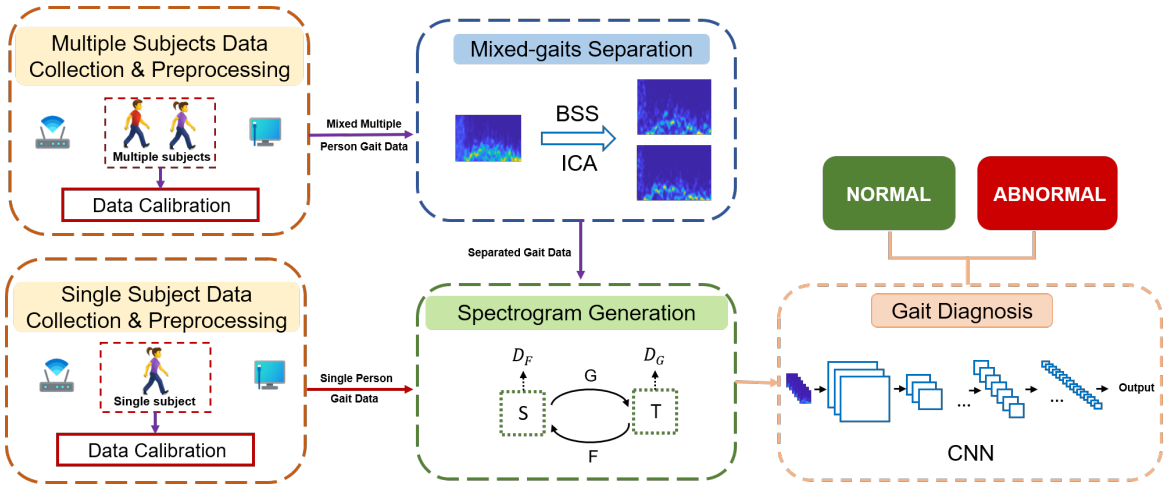

Fig. 1. System overview of Wi-Diag. Wi-Diag contains four modules: data collection and pre-processing, mixed-gaits separation, spectrogram generation, and gait diagnosis.

extracted by autocorrelation of the spectrograms. In WiAU [16], gait information is utilized for user authentication, which requires the individual to walk along a predefined path. An automatic segment algorithm (ASA) and ResNet network are used for feature extraction. WiDIGR [12] uses CSI information to realize gait recognition when subjects walk in a straight line in any direction and removes the directional dependence constraints. It can recognize subjects based on their gait pattern, irrespective of their path. In a word, current commercial Wi-Fi based gait recognition systems are defined in single-subject scenarios.

B. Wi-Fi based Multi-subject Sensing System

Currently, many sensing systems study the scenario of a single subject. That is because the CSI measurements are mixtures of multiple people's movements. It is nontrivial to separate each subject's movement pattern from the mixed signals. Recently, there are great advances in Wi-Fi based multi-subject sensing systems. Wi-Run [27] explores the potential of separating CSI dynamics induced by multiple runners during running, which is validated theoretically and experimentally. In PhaseBeat [28], multiple subjects' breathing and heartbeat are monitored by extracting the phase difference feature between two commercial Wi-Fi antennas and using it in algorithm [29]. In [30], the placement of Wi-Fi devices is optimized carefully leveraging the Fresnel zone theory [31], [32]. Therefore, only one subject influences each CSI stream and the breathing of multiple subjects is detected simultaneously. In WiMU [33], by comparing experimental samples with virtual samples, WiMU achieves multi-user gesture recognition, making it possible to identify gestures made by multiple users simultaneously. WiCrowd [17] simultaneously achieves crowd counting and estimation of walking direction in various environments using a single Wi-Fi link, utilizing augmented feature representations for infinite crowd counting.

In IMar [34], a WiFi-based multi-user action recognition system is proposed. In this work, tensor decomposition is leveraged to derive each individual's activity induced CSI dynamics. In [35], MultiTrack enables simultaneous tracking and recognition of activities for multiple subjects using WiFi. The individual signal reflections from multiple WiFi links and all available 5GHz channels are extracted. In [36], a novel system utilizes estimated breathing rates for subject recognition and people counting. It employs adaptive subcarrier combination, iterative dynamic programming, and trace concatenation to track multiple subjects' breathing rates. In [37], Wi-Multi recognizes multiple human activities. It employs three phases based on the available samples: dynamic time warping (DTW) for a few samples, support vector machine (SVM) for representative feature extraction, and recurrent neural networks (RNN) for a large number of samples. So far, there is no work studying the multiple subjects' disease diagnosis through the gaits. Our work is the first one of multi-subject abnormal gait detection through one pair of commercial Wi-Fi devices.

III. System Design

Wi-Diag is the first Wi-Fi based multi-subject abnormal gait diagnosis system that can accurately distinguish abnormal from normal gaits. In this section, the Wi-Diag system shown in Fig.1 is introduced module by module. There are four basic modules: data collection and preprocessing, mixed-gaits separation, spectrogram generation, and gait diagnosis.

The data collection and preprocessing module, whether for a single subject or multiple subjects environment, collect the CSI measurements, which are preprocessed by applying calibration and walking detection. In the mixed-gaits separation module, The multiple individual gaits separation problem is formulated as a Blind Source Separation (BSS) issue, which can be solved by the ICA algorithm. In the spectrogram generation module, the spectrogram enhancement and transformation are used to generate a high-quality spectrogram. A CycleGAN network is trained by unmixed spectrograms in a multi-subject environment and spectrograms in a single-subject environment. With the trained CycleGAN network, data from other domains can be converted to the domain for gait diagnosis, reducing environmental dependence. In the gait

diagnosis module, the improved spectrograms from a single-subject environment are input into the trained Convolutional Neural Network for gait diagnosis.

A. Data Collection and Pre-processing

1) Data Collection and calibration: Wi-Fi CSI measurements have a significant challenge for activity recognition due to excessive noise. These measurements fluctuate even in environment without human presence, as CSI measurements are vulnerable to surrounding electromagnetic interferences. Furthermore, the CSI measurements are susceptible to impulse and burst noises caused by internal state changes in Wi-Fi transceivers, such as transmission rate and power adaptation. The research presents a two-level denoising technique employing a Butterworth bandpass filter and principal component analysis (PCA), aiming to maintain the valuable information in the CSI measurements effectively. Firstly, the effective walking-induced frequency changes range from 10 to 70 Hz [13], [14]. A Butterworth bandpass filter with a weighted moving average is utilized to do the data calibration. Secondly, the principal component analysis (PCA) is introduced, capitalizing on the correlation among signals across all CSI subcarriers. In summary, PCA presents two significant advantages. On the one hand, it reduces computational complexity by reducing the dimensionality of measurements obtained from the 30 subcarriers in each TX-RX antenna pair while preserving crucial gait information. On the other hand, PCA can effectively eliminate in-band noise. This advantage is based on the correlation in the CSI dynamics caused by human motion across all subcarriers, whereas noise lacks such correlation. The first principal component is chosen, and the normalization is leveraged after PCA to make the amplitude between 0 and 1 as follows:

$$y_i^j = \frac{x_i^j - min\ x_i}{max\ x_i - min\ x_i}; \tag{1}$$

where i denotes the value of principal components, j is the index of samples, the vector before normalization is denoted by x, and y represents the vector after normalization. The utilization of normalization serves to accelerate the convergence of the decision function.

2) Walking Detection: After calibrating the data, a movement detection approach based on the threshold is implemented. When a person is in motion, the signals the body reflects fluctuate more dramatically than when they are stationary. The noise level is tracked by utilizing a dynamic threshold method. To update the noise status value L_t precisely, in particular, we utilize an Exponential Moving Average approach.

$$L_t = (1-\beta)L_{t-1} + \beta \times var_t \tag{2}$$

where β is experimentally determined at 0.1. In the first PCA component, the variance var_t for the i^{th} sliding window consisting of 200 samples is determined. In case the variance var_t within a sliding window differs from the average noise level, the detection threshold is increased to four times the noise level L_t. This approach ensures the accurate detection of any significant deviation from the noise level.

Fig.2 illustrates the deviation in CSI amplitude variance during continuous activities, in which an individual traverses LoS and returns, and the related activities are labeled. The horizontal axis represents time, and the vertical axis represents the square of the variance. When the subject crosses LOS, the variance difference shows a state transition, which is consistent with the previous theory. While the subject stops to stand, there is a significant drop in the variance,which meets our previous detection criteria. In this way, walking detection is performed.

B. Mixed-gaits Separation

In multi-subject case, the additive effect has a detrimental influence on the signals received. In addition, received signals reflected by distinct limbs, which move at various rates, are combined at the receiver. Due to the complex characteristics, conventional techniques that rely on a limited number of Wi-Fi transceivers face difficulty separating each subject's movement-induced gaits. This can be reduced to the Blind Source Separation (BSS) issue. Therefore, to distinguish each subject's gait, Independent Component Analysis (ICA) approach is adopted.

1) Blind Source Separation: This issue is where both the sources and mixing methods are unclear, and only mixed signals are accessible for further separation. Assume that the number of active source signals is a known quantity. The separation is achieved by determining disjoint basis sets for different sources. Assume there are n independent signal sources $s_i(t)$, and multiple people's walking induced signals are the composition of m sets of linear signal combinations $x_j(t)$. The combined signals are expressed as the following at the given time t:

$$x_j(t) = \sum_{i=1}^{M} a_{ji} s_i(t), 1 \le i \le n, 1 \le j \le m \tag{3}$$

where a_{ji} denotes mixing parameter of $x_j(t)$, in terms of vectors:

$$\mathbf{x}(t) = \mathbf{A}\mathbf{s}(t) + \mathbf{n} \tag{4}$$

where $\mathbf{x}$ and $\mathbf{s}$ represent mixture signal vector and source signal vector, $\mathbf{A}$ denotes an unknown $m \times n$ constant mixing parameter matrix, and $\mathbf{n}$ denotes additive channel noise that can be removed from the signal. where

$$\begin{aligned} \mathbf{s(t)} &= \begin{bmatrix} s_1(t), & s_2(t), & \cdots, & s_n(t) \end{bmatrix}^T, \\ \mathbf{x(t)} &= \begin{bmatrix} x_1(t), & x_2(t), & \cdots, & x_m(t) \end{bmatrix}^T, \end{aligned} \tag{5}$$

The fundamental problem of BSS is to determine a corresponding $n \times m$ demixing matrix $\mathbf{W}$ and make the mixed signals separation as complete as possible. $\mathbf{y}$ is an estimated Independent Component (IC) and by $\mathbf{W}$ the corresponding demixing vector,

$$\mathbf{y}(t) = \mathbf{W}\mathbf{x}(t) \tag{6}$$

where $\mathbf{y(t)} = \hat{\mathbf{s(t)}}$ denotes the estimated vector of source signals and the matrix $\mathbf{W} = \hat{\mathbf{A}^{-1}}$ and $\mathbf{A}$ are inverse matrices of each other. Therefore, the demixing matrix W is got and BSS can be applied to derive each subject's walking induced CSI dynamics.

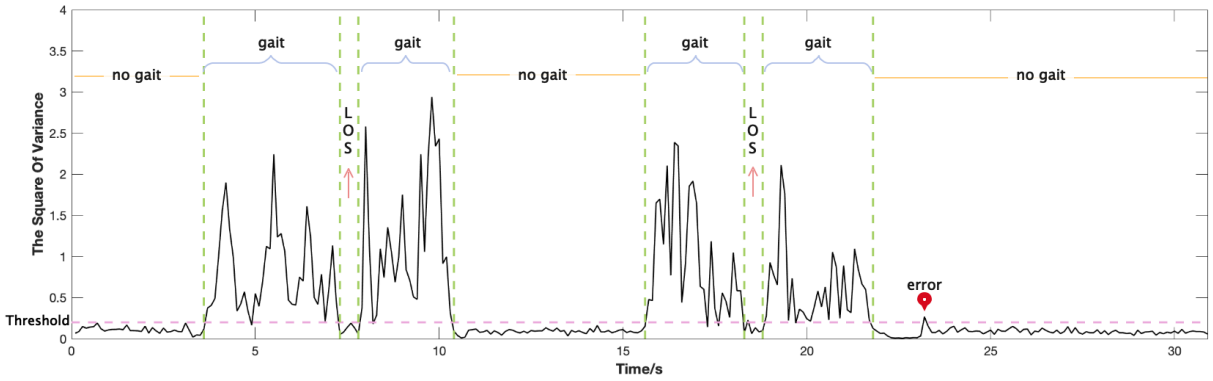

Fig. 2. Walking Detection is implemented by a movement detection based on a threshold. When the subject goes across LOS, the variance change shows a state transition. When the subject stops, there is a significant drop in the variance.

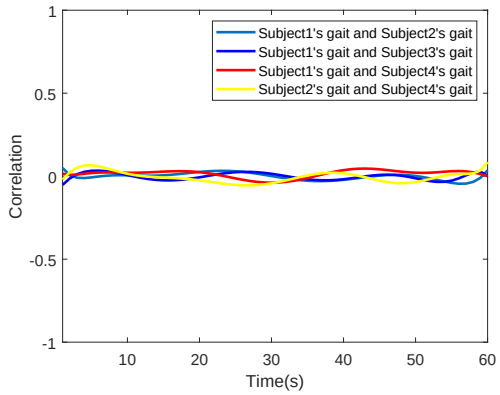

Fig. 3. Correlation between two walking subjects. The different colors represent different groups of subjects.

The ICA (Independent Component Analysis) could be adopted to solve the BSS issue when three conditions are met [38]: Firstly, the source signals are statistically independent. Secondly, the source signals are non-Gaussian. Thirdly, the mixture of source signals can be linearly combined. In the following section, we will examine if the three conditions are satisfied.

2) Condition Check: In this section, we check whether mixed-gaits separation satisfies the three conditions for using Independent Component Analysis (ICA). The BSS issue could then be resolved by utilizing the ICA.

a) Independence of the Sources: Firstly, the independence of the multiple subjects' walking induced CSI dynamics is verified. That is to say, we need to examine the independence of the potential signal sources. Every two subjects are asked to walk, and Kinect 2.0 captures their walking motions as the ground truth. The acquired walking motions are divided into segments that do not overlap. The correlation between two subjects' walking motions throughout each segment is then calculated. This process is repeated for every two subject pairs. Fig.3 shows the correlation between the walking movements of any two subjects. The horizontal axis represents time, the vertical axis represents correlation, and different colors represent different pairs of subjects. The correlation between walking movements of any two subjects is less than 0.05. Therefore, we can prove that each subject's walking movements are independent to the other's.

b) Non-Gaussianity of the Sources: Secondly, the one subject's walking induced CSI dynamic distribution is shown as Fig.4. The distributions are provided based on three antennas at the receiver. During the time, the walking induced CSI amplitudes are processed by the Butterworth filter and PCA. In Fig.4, for each antenna, X values are the sensing results after the Butterworth filter and PCA. Y values are the number of subcarriers whose sensing results after processing fall in the corresponding categories. Clearly the distribution is not Gaussian.

c) Linearity of Observations: Finally, it is verified that the captured CSI dynamics are linear mixtures of walking induced signals. A random transmitter and receiver antenna pair is selected. The CSI measurements received are expressed as follows:

$$x_1(f,t) = e^{-j\psi(t)}(\sum_{i=1}^{N} a_{1,i} \cdot m_i(f,t) + s_1), \tag{7}$$

$$x_2(f,t) = e^{-j\psi(t)}(\sum_{i=1}^{N} a_{2,i} \cdot m_i(f,t) + s_2), \tag{8}$$

where $a_{1,i} = A_{1,i}$, $a_{2,i} = A_{2,i} \cdot e^{-j2\pi \frac{d_{2,i}(t) - d_{1,i}(t)}{\lambda}}$ are related to the amplitude. The difference in reflected path length between each pair of antennas, denoted as $d_{2,i}(t) - d_{1,i}(t)$, can be regarded as invariant. $m_i(f,t) = e^{-j2\pi \frac{d_{1,i}(t)}{\lambda}}$ represents the body motion signal. This process can be applied to all the CSI antenna pairs. The conclusion is that the walking-induced CSI dynamics of both subjects are linearly combined with the motion signals $m_i(f,t)$ and the environment static signals $s_i (i = 1, 2, \ldots, N)$.

The remaining antenna pairs' linearity are examined. For each receiving antenna, the signals reflected from two walking subjects are linearly combined. In addition, all CSI measurements can be expressed as follows:

$$\boldsymbol{x}(f,t) = e^{-j\psi(t)}(\boldsymbol{A}\boldsymbol{m}(f,t) + \boldsymbol{s}) \tag{9}$$

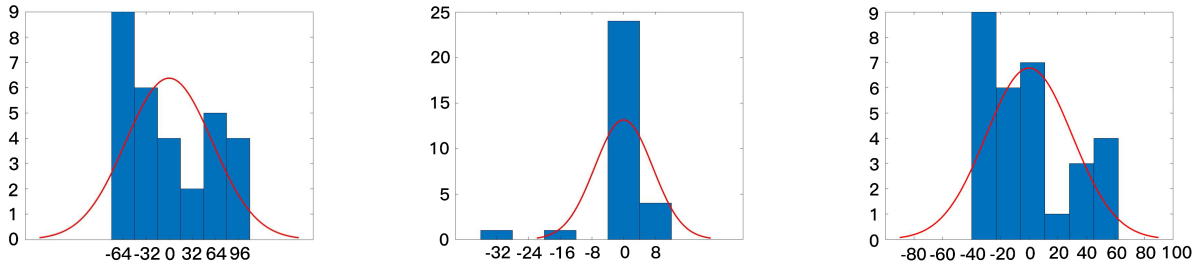

(a) For the first antenna,the number of subcarriers whose sensing results fall in the different CSI amplitude value categories after the Butterworth filter and PCA.

(b) For the second antenna,the number of subcarriers whose sensing results fall in the different CSI amplitude value categories after the Butterworth filter and PCA.

(c) For the third antenna,the number of subcarriers whose sensing results fall in the different CSI amplitude value categories after the Butterworth filter and PCA.

Fig. 4. The CSI amplitude distribution on each antenna is non-Gaussian.

where $\boldsymbol{x}(f,t) = [x_1(f,t)\ x_2(f,t)\ \ldots\ x_M(f,t)]^T$ denotes CSI values of each antenna pair, $\boldsymbol{A}$ denotes a matrix with dimensions $M \times N$, $\boldsymbol{m}(f,t) = [m_1(f,t)\ m_2(f,t)\ \ldots\ m_M(f,t)]^T$ marks CSI signals induced by walking motion and $s = [s_1\ s_2\ \ldots\ s_M]^T$ denotes static signals.

Owing to the phase distortion of commercial Wi-Fi devices, obtaining the phase information from the raw CSI signals is difficult. To maintain the linearity of walking-induced CSI dynamics, it is necessary to process the phase shift so that it can be utilized. To calibrate and maintain the linearity of the CSI, the conjugate multiplication [39] is adopted.

A key characteristic exploited here is that all antennas on a Wi-Fi card use the identical RF oscillator, which leads to time-variant random phase offsets that are identical on all antennas [40], [41]. Hence, the conjugate multiplication is leveraged to eliminate the CSI phase errors and maintain the linearity.

$$
\begin{aligned}
x_{cm}(f,t+\Delta t) &= x_1(f,t+\Delta t)\overline{x}_2(f,t+\Delta t) \\
&= (x_{1,s}(f,t) + \sum_{i\in D_1} a_{1,i}e^{-j2\pi f(\tau_i+\frac{v_i\Delta t}{c})}) \\
&\times (\overline{x}_{2,s}(f,t) + \sum_{k\in D_2} a_{2,k}e^{j2\pi f(\tau_k+\frac{v_k\Delta t}{c})}) \\
&= \overbrace{x_{1,s}(f,t)\overline{x}_{2,s}(f,t)}^{①} \\
&+ \overbrace{\sum_{i\in D_1,k\in D_2} a_{1,i}a_{2,k}e^{-j2\pi f((\tau_i-\tau_k)+\frac{(v_i-v_k)\Delta t}{c})}}^{②} \\
&+ \overbrace{\overline{x}_{2,s}(f,t)\sum_{i\in D_1} a_{1,i}e^{-j2\pi f(\tau_i+\frac{v_i\Delta t}{c})}}^{③} \\
&+ \overbrace{x_{1,s}(f,t)\sum_{k\in D_2} a_{2,k}e^{j2\pi f(\tau_k+\frac{v_k\Delta t}{c})}}^{④}
\end{aligned}
\tag{10}
$$

where $x_{cm}(f,t+\Delta t)$ denotes the result of conjugate multiplication, $x_1(f,t+\Delta t)$ and $\overline{x}_2(f,t+\Delta t)$ denotes the CSI value of one antenna and the CSI conjugate value of the other antenna, respectively. D_1 and D_2 represent the corresponding sets of moving paths at both antennas.

The combination of static paths part from two received antennas, denoted as ① in Equation (10), is regarded invariable during a short period and does not include dynamic information. The strength of the static part is relatively high due to the strong Line of Sight (LoS). Therefore, we deduct the mean value from $x_{cm}(f,t+\Delta t)$ to eliminate the static component.

The combination of the dynamic path parts, denoted as ②, is so tiny that it can be ignored. The ③ and ④ represent the two combinations of the static-path part from one antenna and the dynamic-path part from the other. The motion-related information is included in these two parts. Due to the similar reflection path of two nearby antennas, the dynamic parts of the two antennas are identical in value and opposite in direction. The dynamic information is acquired by multiplying the dynamic paths part of one antenna by the static paths part of another antenna, denoted as ③. Therefore, adding a weight α on the first antenna and β on the second antenna can reduce the first antenna's static path attenuation while increasing the second antenna's static path attenuation.

After adjustment, the effect of ④ has been reduced enough to be negligible as the ② and the ③ plays an absolutely dominant role in the result of the conjugate multiplication. So this indicates that the CSI data processed still maintain the characteristic of linearity combination between source signals (i.e., different subjects' motion signals). As a result, the ICA can be adopted to achieve multi-subject signal separation.

3) Independent Component Analysis: Here, the RobustICA method [42] is adopted due to its characteristic of handling complex-valued signals and rapidly converging. The output of the RobustICA is multiple subjects' complex-valued walking-induced CSI dynamics.

Fig.5 depicts an example of walking signal separation of double subjects by RobustICA. The dots donate CSI data collected over time, and the lines present one after being processed by the Savitzky-Golay filter. Fig.5(a) and 5(b) illustrate processed CSI measurements about double subjects in two antenna pairs. Fig.5(c) and Fig.5(d) demonstrate outputs after using the RobustICA algorithm. It is obvious that the data distribution trends of two subjects' separated walking induced signals rotate counterclockwise in the complex plane.

This article has been accepted for publication in IEEE Internet of Things Journal. This is the author's version which has not been fully edited and content may change prior to final publication. Citation information: DOI 10.1109/JIOT.2023.3301908

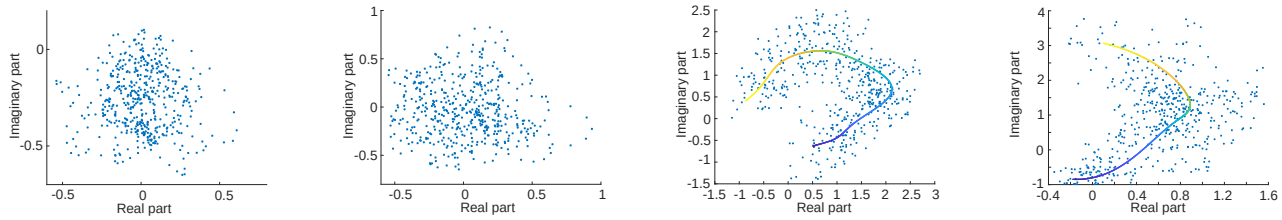

Fig. 5. Two subjects' walking induced CSI dynamics separation. (a) the CSI measurements of the first antenna pair; (b) the CSI measurements of the second antenna pair; (c) the separated measurements of the first subject; and (d) the separated measurements of the second subject.

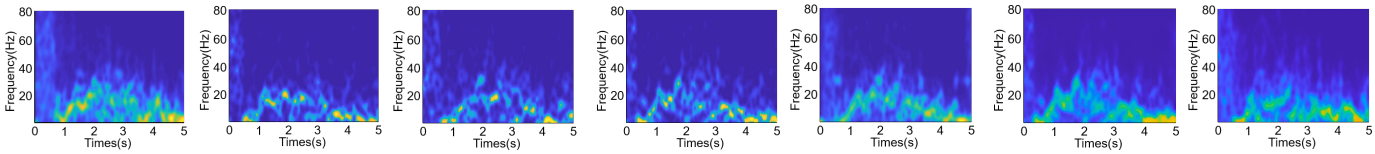

(a) Two subjects walking induced CSI mixtures generate a spectrogram.
(b) Subject A's spectrogram after ICA separation.
(c) Subject B's spectrogram after ICA separation.
(d) Subject A's spectrogram after enhancement.
(e) Subject B's spectrogram after enhancement.
(f) Subject A's spectrogram after transformation.
(g) Subject B's spectrogram after transformation.

Fig. 6. Two subjects' walking generated spectrogram changes after each processing: ICA separation, spectrogram enhancement and spectrogram transformation.

As proposed in [43], this indicates both subjects move towards the transmitter-receiver pair.

C. Spectrogram Generation

There are various frequencies in all body parts due to the radio signals reflected. Therefore, we convert CSI measurements into the frequency domain to obtain separable frequency distributions. The CSI measurements taken at different speeds across various frequencies are processed with denoising and PCA techniques and then transformed into the time-frequency domain using the Short-Time Fourier Transform (STFT) method to contribute to extracting feature better. Here, the CSI measurement waveforms are transformed into spectrograms in the time-frequency domain. A sliding window technique is employed to divide the CSI measurement waveform into segments, each of which is then subjected to the Fast Fourier transform (FFT) to produce a corresponding spectrogram, which consists of the time axis, frequency axis and CSI amplitude power axis. The time and frequency resolutions of STFT are defined through the sliding window technique. The STFT offers improved frequency resolution but decreased temporal resolution when the window size is increased. An average human walking frequency ranges from 20Hz to 40Hz and changes rapidly. To better track the change in walking signal frequency, we specified the FFT window size as 1024 and the sliding step as 1. As presented in Fig.6(a), the hotter color corresponds to greater FFT amplitude. The heat maps after applying the ICA algorithm are provided in Fig.6(b) and Fig.6(c).

1) Spectrogram Enhancement: After spectrogram generation, the spectrogram enhancement technique is applied. Firstly, the energy level for all chunks is calculated by totaling the magnitudes of the first 100 samples. The ones whose energy level is less than an experience threshold are disregarded, and the silence intervals are deleted. The magnitude of the FFT for all remaining chunks is normalized by dividing their energy level. Secondly, the spectrogram in the frequency domain is denoised by removing noise, which is calculated by averaging the spectrogram over a short period. After this processing, if the magnitude becomes negative, it will be assigned to 0. Thirdly, the spectrograms from the top 20 PCA results are superimposed, which is achieved by summing the magnitude of the corresponding blocks. Fourth, we utilize a two-dimensional Gaussian low-pass filter to further filter noise, with a size of 5 and σ of 0.8. Finally, a transformed high-quality spectrogram is generated. The spectrograms after enhancement are provided in Fig.6(d) and Fig.6(e).

2) Spectrogram Transformation: As illustrated in [22], the major challenge of abnormal gait distinction is that Wi-Fi signals received often contain considerable information particular to the environment in which the activity is performed. A well-trained abnormal gait classification model in a typical scenario may not be suitable for another scenario. This is referred to as the environment dependency of the recognition model. In the Wi-Diag system, the spectrogram transformation is to mitigate the environment dependency from the spectrogram aspect. Specifically, the spectrogram transformation is essentially image conversion by learning the mappings of both input and output images via training sets that align image pairs.

An important application area for CycleGAN is "Domain Adaptation" [44]. The recent advances in the CycleGAN demonstrate its impressive performance on image transformation tasks [44], [45], [46], [47]. In the Wi-Diag system, by adopting the CycleGAN model, the gait information of one subject in one domain can be transformed into the same subject's gait information in the other domain while keeping the gait information consistent across various domains. The separated gait features in the multi-subject scenario are do-

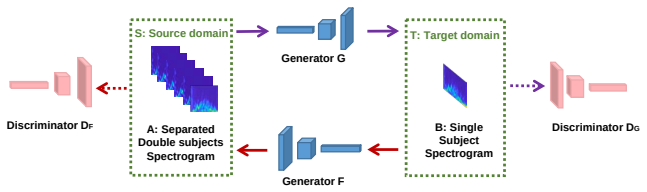

Fig. 7. Framework of the CycleGAN. The framework comprises two mappings, $G : S \rightarrow T$ and $F : T \rightarrow S$, and two adversarial discriminators, D_F and D_G.

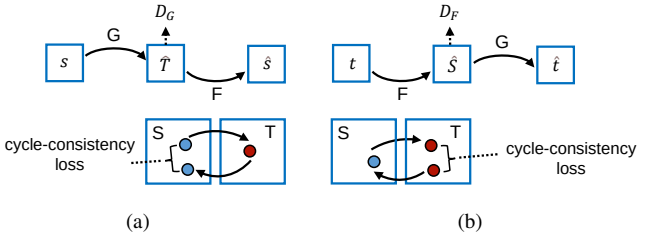

Fig. 8. Cycle Consistency Loss. (a) Forward Cycle-Consistency Loss: $s \rightarrow G(s) \rightarrow F(G(s)) \approx s$ and (b) Backward Cycle-Consistency Loss:$t \rightarrow F(t) \rightarrow G(F(t)) \approx t$ [44].

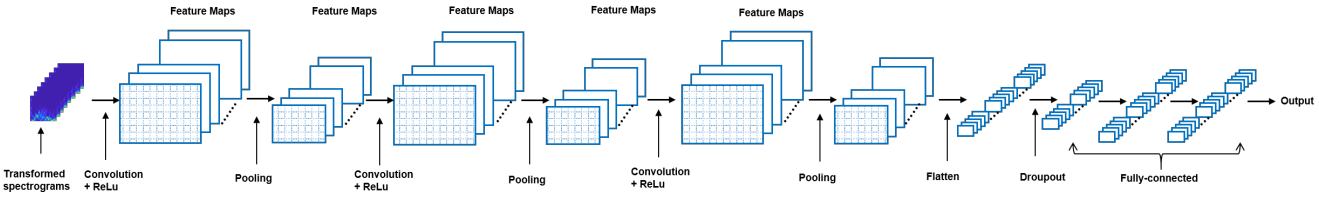

Fig. 9. CNN classifier network structure.

nated as the source domain S. Each subject's gait features in the single subject scenario are donated as the target domain T. In Fig.7, generator G transforms spectrogram A from source domain S into spectrogram B in target domain T. Then, the spectrogram B is converted back to the spectrogram A of the source domain by generator F. CycleGAN model is trained by discriminator D_G and D_F. The unsupervised CycleGAN [44] can automatically match the separated spectrograms to the most appropriate gait spectrogram in the single target environment. In the end, a relatively effective data generator generating new samples for the target domain is obtained. So far, in the new environment, a small mount of single subject gait information is collected, and a certain mount of the gait information is generated by the CycleGAN. In this way, environmental dependence is mitigated by domain adaptation.

a) Formulation: The purpose is to learn how to map two S and T domains with training data sets $\{s_i\}_{i=1}^{N}$ and $\{t_j\}_{j=1}^{M}$, where $s_i \in S$, $t_j \in T$. The data distributions are $s \sim p_{data}(s)$ and $t \sim p_{data}(t)$. As depicted in Fig.7, the framework comprises two mappings, $G : S \rightarrow T$ and $F : T \rightarrow S$, and two adversarial discriminators, D_F and D_G, that work in tandem to achieve the desired outcome. The D_F seeks to discriminate both spectrograms $\{s\}$ and transformed spectrograms $\{F(t)\}$; similarly, D_G seeks to differentiate both $\{t\}$ and $\{G(s)\}$. The loss function includes two components: Adversarial Loss and Cycle Consistent Loss. The Adversarial Loss is to narrow the difference between the generated images by the generator and the actual images. In addition, the Cycle Consistency Loss ensures consistency is maintained before and after the transformation using the two mappings.

b) Adversarial Loss: It is utilized to train two generators to produce high-quality images indiscernible from real images. The loss function with regards to $G : S \rightarrow T$ and corresponding discriminator D_G can be formulated as follows:

$$\min_{G} \max_{D_G} \mathcal{L}_{\text{GAN}}\left(G, D_G, S, T\right) = \mathbb{E}_{t \sim p_{\text{data}}(t)}\left[\log D_T(t)\right] + \mathbb{E}_{s \sim p_{\text{data}}(s)}\left[\log\left(1 - D_G(G(s))\right)\right] \tag{11}$$

where G tries to composite spectrograms $G(s)$ that resemble spectrograms in domain T, and D_G attempts to differentiate both transformed images $G(s)$ and actual images t. G tries to minimize losses, while D does the opposite to improve the system's overall performance. The loss function for $F : T \rightarrow S$ and its corresponding discriminator D_F are comparable in nature, and that is: $\min_F \max_{D_F} \mathcal{L}_{\text{GAN}}\left(F, D_F, T, S\right)$.

c) Cycle Consistency Loss: The cycle consistency narrows the possible mappings set that network can learn, and forces mapping functions F and G to perform opposite transformations to achieve meaningful mappings. In Fig.8(a), the spectrogram transformation cycle is capable of transforming all spectrograms s from the domain S to the source spectrograms, in other words, $s \rightarrow G(s) \rightarrow F(G(s)) \approx s$. It is called the Forward Cycle Consistency. In a similar way, Fig.8(b) demonstrates that for all corresponding spectrograms t in T, G and F satisfy the Backward Cycle Consistency condition: $t \rightarrow F(t) \rightarrow G(F(t)) \approx t$. Therefore, the Cycle Consistency Loss is utilized as an incentive for the process.

$$\begin{aligned}\mathcal{L}_{\text{cyc}}(G, F) = \mathbb{E}_{s \sim p_{\text{data}}(s)}\left[\|F(G(s)) - s\|_1\right] \\ + \mathbb{E}_{t \sim p_{\text{data}}(t)}\left[\|G(F(t)) - t\|_1\right].\end{aligned} \tag{12}$$

where $\|\cdot\|_1$ is the L1 norm.

d) Full Objective: The overall loss as following:

$$\begin{aligned}\mathcal{L}\left(G, F, D_F, D_G\right) = \mathcal{L}_{\text{GAN}}\left(G, D_G, S, T\right) \\ + \mathcal{L}_{\text{GAN}}\left(F, D_F, T, S\right) \\ + \lambda \mathcal{L}_{\text{cyc}}(G, F)\end{aligned} \tag{13}$$

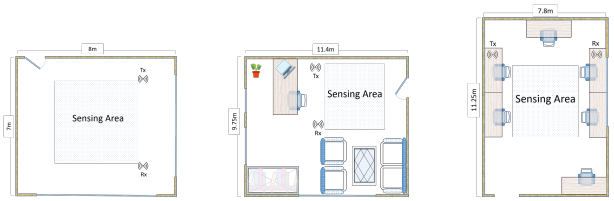

(a) Empty hall. (b) Office. (c) Lab.

Fig. 10. The layouts of three typical scenarios. The location of the transceivers and the sensing areas are marked in all the figures.

where λ determines the weight distribution of these two loss functions. In order to achieve the following:

$$G^*, F^* = \arg\min_{G,F} \max_{D_F, D_G} \mathcal{L}\left(G, F, D_F, D_G\right). \quad (14)$$

The framework can be thought as two "autoencoders": one $F \circ G : S \rightarrow S$ and the other $G \circ F : T \rightarrow T$. The two autoencoders are implemented by transforming the spectrograms to an intermediate state in another domain and then mapping it to themselves.

e) Network Architecture: The network architecture is derived from [48], including three convolution layers, two fractionally strided convolution layers with stride value being one, three residual blocks, and the last convolution layer mapping feature extracted to images. Meanwhile, normalization [49] is leveraged. The 70 $\times$ 70 PatchGANs structure [50] is utilized in discriminator network structures, which can handle spectrograms of any size with fewer parameters. The training dataset for the network consists of 513 spectrograms from the source domain and 452 spectrograms from the target domain respectively. Fig.6 (f)(g) show the spectrogram transformations corresponding to Fig.6 (d)(e).

D. Gait Diagnosis

The convolutional neural network (CNN) can have better performance in classification compared with the traditional classifiers since it can automatically extract more comprehensive features. Wi-Diag utilizes CNN as the classifier. The disease diagnosis model CNN is trained with CSI gait samples obtained in the single subject scenario so that it can be applied to identify abnormal gaits from the separated spectrograms. The network structure is shown in Fig.9.

IV. EXPERIMENTS AND EVALUATION

A. Prototype and Experiment Setting

1) Hardware setup: In Wi-Diag, the Linux 802.11n CSI Tool [51] is used on an Ubuntu desktop 14.04 LTS operating system, and two ThinkPad T-series laptops with Intel 5300 NICs are employed. One of the laptops, fitted with a single antenna, functioned as the transmitter. While the other, outfitted with three external antennas, served as the receiver. All the devices utilized in Wi-Diag are equipped with external antennas for easier deployment. The sender and receiver are positioned on the floor with a distance of 4m between them and operate on Channel 161 at 5.825 GHz in IEEE 802.11n monitor mode. The multiple antennas are arranged adjacently in a horizontal line at the receiver, with a wavelength interval between them. Each antenna at the receiver obtains 30 streams, for a total of 90. The transmitter power is set to 15dBm, and so does the receiver power. The packet transmission rate is 1000Hz. MATLAB is used to analyze the CSI readings.

2) Experimental dataset: As presented in Fig.10, Wi-Diag is evaluated in three common scenarios: (i) an empty hall, (ii) an office, and (iii) a lab. The empty hall measures about $7m \times 8m$ in size. Ninety-six participants, including 48 men and 48 women, are evaluated with Wi-Diag for three months. The participant's age, height, and weight distributions are as follows: 20 to 60 years old, $155cm$ to $185cm$ in height, and $44kg$ to $80kg$ in weight. Gait information in a single-subject environment and a multi-subject environment are collected. The experiment participants are asked to learn various abnormal walking patterns (such as Spastic gait, Scissors gait, Steppage gait, Parkinsonian gait, etc.) [6], [7] through video before the experiments. During the experiments, each participant randomly selects a gait pattern (normal or abnormal as TABLE I) to walk.

In the single-subject data collection, each subject walks naturally in an identical straight-line route 30 times, including 15 times for normal and 15 times for abnormal gaits. Abnormal gaits are collected mainly by imitating abnormal gait patterns (such as Spastic gait, Scissors gait, Steppage gait, Parkinsonian gait, etc.), as shown in TABLE I. The walking distance is about $5m$. And in a multi-subject data collection, multiple subjects are tested in a group in all three scenarios. Subjects in each group are randomly selected from 96 participants. The group size varies from two to four subjects. Each randomly selected group does the experiment 30 times. Each group walks in an identical straight-line route 10 times. The participants start walking simultaneously and walk in parallel along the same $5m$ length path. The path is perpendicular to LoS. HD videos are recorded as the ground truth.

3) Training details: The training dataset for CycleGAN comprises 513 spectrograms from the source domain and 452 spectrograms from the target domain with an image size of 128 $\times$ 256. During training, λ is set to 10 in Equation (13), and the Adam solver [52] is utilized with the stride value being 1. The network is configured with a learning rate of 0.001.

In the "Disease Diagnosis" module, the CNN network is trained with 2,880 labeled CSI measurements (96 users $\times$ 2 conditions $\times$ 15 instances) from the single subject environment, including normal and abnormal gait measurements. The input spectrograms are of size 128 $\times$ 256, and the network is configured with a learning rate of 0.001. The CSI gait measurements of multiple subjects in a multi-subject environment are collected and calibrated. The ICA algorithm is leveraged to separate the mixture signals of multi-subject walking. The spectrogram transformation is applied to mitigate environmental dependency. Finally, CNN is utilized to diagnose abnormal gaits. Five hundred randomly selected spectrograms are used for testing in each domain.

4) Experimental Metrics: True Positive Rate and False Positive Rate are used to test the performance of Wi-Diag. TPR is the proportion of all normal condition samples where the prediction is correct to all normal condition samples.

TABLE I
ABNORMAL GAIT TYPES AND CORRESPONDING DESCRIPTIONS [7].

Abnormal gait type	*Descriptions*
Spastic gait	A spastic gait manifests as dragging the feet when walking. The lower limbs can remain extended throughout due to high muscle tone.
Scissors gait	An individual exhibiting inward leg bending presents a scissors gait. This gait exhibits a crossing pattern and may collide with each other during walking.
Steppage gait	The downward pointing of toes characterizes steppage gait during walking. The toes often brush against the ground while forward steps.
Waddling gait	Waddling gait A waddling gait is characterized by a side-to-side movement while walking. Waddling contains combining short steps and a swinging body.
Propulsive gait	Propulsive gait is characterized by the forward positioning of the head and neck while walking. The individual may appear rigid and slouched while maintaining the propulsive gait.
Parkinsonian gait	The patient often exhibits forward bending of the head and neck and flexion of the knees. The patient takes small steps when walking and may exhibit involuntary forward leaning.

$$TPR = \frac{TP}{TP + FN} \tag{15}$$

FPR refers to the proportion of all abnormal condition samples where the prediction is incorrect for all abnormal condition samples.

$$FPR = \frac{FP}{TN + FP} \tag{16}$$

Accuracy(ACC) is the proportion of samples correctly predicted out of the total number of samples across all experiments.

$$ACC = \frac{TP + TN}{TP + TN + FP + FN} \tag{17}$$

where TP, TN, FP, and FN denote the number of true positives, true negatives, false positives, and false negatives, respectively. The experimental results are the mean of different test individuals in the environment.

The Receiver Operating Characteristic (ROC) curve is a commonly used tool for evaluating the performance of a classifier. The ROC curve plots the true positive rate (TPR) on the y-axis versus the false positive rate (FPR) on the x-axis. It can be used to compare the performance of different systems by comparing the area under the curve (AUC). AUC is the area under the ROC curve. The larger the AUC, the better the system performance. AUC values closer to 1 indicate better classifier performance, while values closer to 0.5 indicate poorer performance, and a value of 0.5 indicates performance equivalent to random guessing. Therefore, ROC curves and AUC values are valuable tools for evaluating classifier performance.

B. Overall Performance

Wi-Diag's overall performance is evaluated in three typical settings, as presented in Fig.10. In an empty hall, the single subject's gait information is collected and leveraged to train the diagnostic network model. The separated multi-subject gait information is tested in the single-subject environment.

TABLE II
DIAGNOSIS ACCURACY IN THREE TYPICAL INDOOR SCENARIOS.

Scenario	*Accuracy*
Empty hall	91.20%
Lab	85.69%
Office	86.42%

The results are presented in TABLE II. Wi-Diag behaves differently in various scenarios. The average diagnosis accuracy in the three scenarios is above 85%. Wi-Diag has the highest diagnosis accuracy in the empty hall due to less multipath interference. In the lab and office, Wi-Diag does not perform well. The average abnormal diagnosis accuracies in the lab and office are 85.69% and 86.42%, respectively. The CycleGAN is trained to make the domain adaptation. Specifically, through CycleGAN, the separated multi-subject's walking-induced data in one scenario are transferred to the other scenario. This helps to mitigate the difference among the various domains as well as reduce the training data needed for classification. In other words, the CycleGAN has the capability to maintain gait information consistent across various domains and reduce classifier training overhead. Though more complex layouts and superimposed multipath lead to performance deterioration, the results still show the Wi-Diag's effectiveness for multi-subject abnormal gait diagnosis in various scenarios.

C. Performance Evaluation

1) Performance Comparisons: In three typical indoor scenarios, Wi-Diag compares to the baseline of four Wi-Fi gait recognition systems, i.e., Wi-PIGR [13], WiDIGR [12], WifU [14] and WiWho [15], all of which are used for individual gait recognition. The presented results are the average of the accuracy in each typical scenario. In each test, Wi-Diag uses separated signals for abnormal gait diagnosis. The network does not use testing data during training, and the final results are the average of 500 samples selected randomly in the testing set. As presented in Fig.11, Wi-Diag still has a good performance compared with other systems. Although

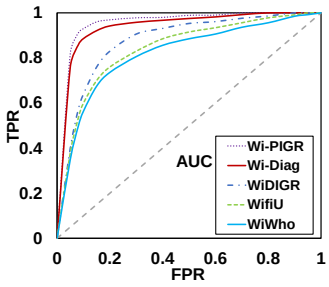

Fig. 11. The comparisons with the other gait recognition systems.

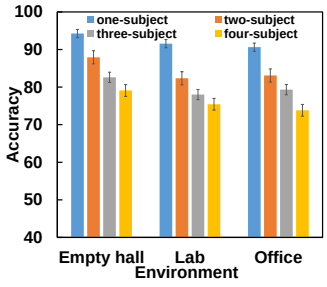

Fig. 12. The impacts of different walking subject numbers on the diagnosis accuracy in various scenarios.

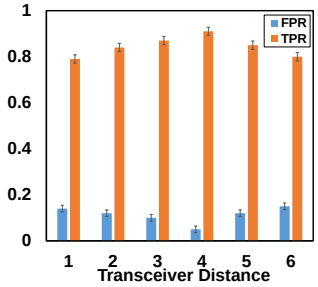

Fig. 13. The impacts of different LoS path lengths (1m $\sim$ 6m).

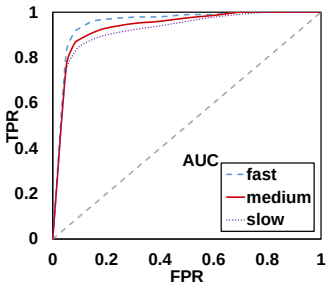

Fig. 14. The impacts of distinct walking speeds (fast,medium,slow).

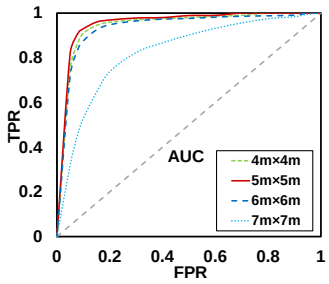

Fig. 15. The impacts of the distinct walking areas (4m $\times$ 4m $\sim$ 7m $\times$ 7m).

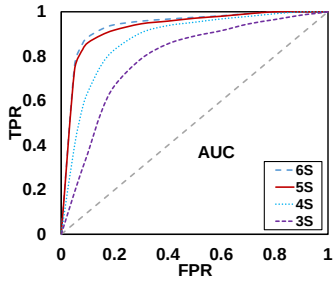

Fig. 16. The impacts of distinct walking time (3s $\sim$ 6s).

its performance is worse than Wi-PIGR, Wi-Diag can still perform well in multiple subjects scenarios.

2) Impact of Subjects and Scenarios: As wireless signals are very sensitive to the environment changes. It is necessary to test the Wi-Diag's performance in various scenarios. Specifically, we train Wi-Diag in the empty hall and test it in the office and lab. The layouts of three environments are illustrated in Fig.10, and group size varies from one to four subjects. Fig. 12 displays the mean accuracy for each environment, where Wi-Diag achieved an overall accuracy of 85.24%, 81.42%, and 80.68% in the empty hall, lab, and office, respectively. In addition, the number of subjects is critical in determining accuracy. As plotted in Fig.12, in all scenarios, one subject always has the highest abnormal gait diagnosis accuracy, and the greater the number of subjects in each group in testing, the lower the diagnostic accuracy. The reason is that when several people walk simultaneously, the reflected signals caused by different subjects will affect each other [19], [53], interfering with the CSI dynamics used for diagnosis. In particular, the CSI dynamic change caused by the walking of one subject overlaps or cancels with that caused by others. It is the reason that leads to the accuracy of abnormal gait diagnosis decrease. Even so, Wi-Diag maintains a mean diagnostic accuracy of 82.45%. With the testing scenario altered, the accuracy of abnormal gait diagnosis degrades somewhat. Based on the results, it can be inferred that the CycleGAN approach utilized in this research can be a promising solution for reducing the environmental dependence on Wi-Fi sensing.

3) Impact of Distinct LoS Path Length: Initially, it is set to 4m as a default. Subsequently, the impact of various LoS lengths is assessed by varying the distance from 1m to 6m in increments of 1m. The results are the average of different group sizes and scenarios. Fig.13 exhibits the result of different LoS lengths under the classifier threshold 0.5. We can observe that the TPR first increases and reaches the highest value when the length is 4m and then decreases gradually with the LoS path length increase. However, FPR is the opposite of TPR. With the increase of LoS length, FPR declines. When the LoS length is set to 4m, FPR reaches the lowest value and rises afterward. That is to say, Wi-Diag performs the best at this distance. These validate experiment results in [54].

4) Impact of Distinct Walking Speed: The average pace v of an ordinary person walking is typically between $1m/s$ and $1.5m/s$, as indicated in [55], [56]. In this study, participants require to walk at three distinct speeds to collect data: (1) high speed(above$(v+0.2)m/s$), (2) normal speed($(v-0.2)m/s \sim (v+0.2)m/s$) and (3) low speed (below $(v-0.2)m/s$). Fig.14 shows the result with the average of different speeds. Even walking at various speeds, Wi-Diag maintains excellent performance of abnormal gait diagnosis. Therefore, walking speed is not a key point influencing performance.

5) Impact of Distinct Walking Area: In this experiment, participants require to walk to collect data at four sensing areas with varying sizes from 4m $\times$ 4m to 7m $\times$ 7m, and all other experimental conditions are consistent. Fig.15 exhibits the result of various walking areas. Wi-Diag can still achieve high abnormal gait diagnosis accuracies while walking areas vary from 4m $\times$ 4m to 6m $\times$ 6m. Nevertheless, the accuracy of abnormal gait diagnosis declines dramatically in 7m $\times$ 7m. When the subjects walk at a distance, the signal propagation distance becomes longer, the signal transmission power declines, the noise increases, and the packet loss is severe, making the long-distance abnormal gait diagnosis challenging. Due to the constraints of the hardware devices, the diagnosable size of Wi-Diag is restricted to 6m $\times$ 6m. To increase the walking area, we can improve the power of the transmitting antenna or strengthen the transmitting signal through signal enhancement.

6) Impact of Distinct Walking Time: Walking time also affects the diagnostic accuracy of abnormal gait. In principle, the longer we walk, the more information we can extract

TABLE III
IMPACTS OF CORE COMPONENTS.

Room	*Empty hall*	*Lab*	*Office*
Without ICA, With CycleGAN	52.32%	48.36%	50.15%
With ICA, Without CycleGAN	87.52%	68.13%	67.32%
ICA + CycleGAN	91.20%	85.69%	86.42%

about gait. To evaluate the influence of different walking times, participants require to walk to collect data at four different times, from 3s to 6s with the step of 1s, and all other experimental conditions are consistent. As illustrated in Fig.16, it is noticeable that as the walking time increases, the improvement in diagnostic accuracy becomes less discernible. Enough time is necessary to reach the best detection accuracy. In addition, the diagnostic accuracy of walking time for both 5s and 6s is similar. Therefore, for the Wi-Diag system, 5 seconds is the optimum time to get the best abnormal gait detection accuracy.

7) Impact of Core Component: In this section, the ablation experiments are conducted on two core components (ICA and CycleGAN). The ICA is adopted to separate each subject's walking induced CSI dynamics from the mixture signals. If ICA is removed, the spectrograms generated by the multi-subject walking induced CSI dynamics will be input into the spectrogram transformation module CycleGAN and the gait diagnosis module CNN. The experiments are done separately in each domain, as shown in Fig.10. TABLE III lists the average diagnosis accuracies with and without ICA. The average diagnosis accuracies without ICA are 52.32%, 48.36%, and 50.15% in empty hall, lab, and office, respectively. The average accuracies with ICA are 91.2%, 85.69%, and 86.42% in empty hall, lab, and office, respectively. It is obvious that ICA has the capability of separating the mixed CSI dynamics induced by multiple subjects' walking so that each subject's CSI dynamics can be derived. Without ICA's separation, each subject's CSI dynamics cannot be derived, the satisfactory diagnosis accuracies cannot be guaranteed. This validates the effectiveness of ICA.

The effectiveness of the spectrogram transformation achieved by CycleGAN is studied. If CycleGAN is removed, each individual gait signals separated by ICA in each domain is directly input into CNN, which is the trained classifier. During the experiments, the spectrograms with transformation and without transformation are input into CNN separately. The experiments are conducted separately in each domain. TABLE III lists the average diagnosis accuracies with and without CycleGAN. The average accuracies with ICA and without CycleGAN are 87.52%, 68.13%, and 67.32% in empty hall, lab, and office, respectively. The average accuracies with ICA and CycleGAN models are 91.2%, 85.69%, and 86.42% in empty hall, lab, and office, respectively. Therefore, there are distinguished differences between the average accuracies with and without CycleGAN. By adopting the CycleGAN model, the gait information of one subject in one domain is transferred to the same subject's gait information in the other domain while keeping the gait information consistent across various domains. By this domain adaptation, the environmental dependence is mitigated. This validates the domain adaptation effectiveness of CycleGAN.

V. DISCUSSION

Wi-Diag shows the feasibility of multi-subject abnormal gait diagnosis using a single pair of commodity Wi-Fi equipment. However, there are still issues with the Wi-Diag system.

A. People interference

When a subject is walking, other people passing by in the sensing region will cause additional interference to the CSI dynamic received at the receiver [57], which will exert a bad influence on the abnormal gait diagnosis. For Wi-Diag, the static subject in the sensing area does not affect the received CSI dynamics. However, for other people irrelevant to subjects in the sensing area of a realistic scenario, the interference signals they generate will also be mixed into the CSI dynamics received by the receiver. It will be challenging to deduce each subject's walking-induced signals because of inherent issues of Wi-Fi hardware devices. The current solution of Wi-Diag can not work effectively, and that's what we will study in the future.

B. Subjects' Number

The ICA approach used in Wi-Diag requires identifying the number of actual test subjects, which is not resolved by the ICA algorithm. Uncertainty about the number of source signals is an intrinsic property of ICA [58]. One possible solution might be integrating a people counting system in the sensing area, such as Wi-Count [59]–[61]. How to effectively tailor the people counting module to the Wi-Diag system is an interesting feature to be included in the future.

C. Path Dependence

In the Wi-Diag system, one constraint is all the subjects must walk along predetermined straight-line routes. While it's ideal to allow subjects to work freely in the indoor environment and get rid of the path dependence issue, this constraint is still acceptable in some medical institutions. Adding an additional Wi-Fi receiver and mitigating path dependence is worth investigating in the future.

D. Abnormal Gait Disease Diagnosis

The diagnostic process of Wi-Diag is a binary classification that can only distinguish the abnormal gaits from the normal gaits and cannot diagnose what kind of abnormal gait disease it is, such as Parkinson's syndrome. In order to make the system more widely used, specific abnormal gait disease type diagnosis might be an interesting topic for our future work.

VI. Conclusion

This paper presents Wi-Diag as a novel approach to assist medical professionals in diagnosing gait-related disorders. It is the first commercial Wi-Fi based system which can effectively separate multiple subjects' gait information utilizing only one pair of off-the-shelf commodity Wi-Fi transceivers. Additionally, Wi-Diag demonstrates its robustness by mitigating environmental dependency. Therefore, it can adapt to the new scenario well. All experiments in various scenarios show that Wi-Diag's mean accuracy is 87.77% even in the presence of four subjects. The theory behind Wi-Diag is that the multi-subject abnormal gait diagnosis could be formulated as a BSS problem and be tackled by the ICA algorithm. This is definitely a great advance for commercial Wi-Fi based multi-subject sensing. Wi-Diag is a great progress toward a practical contactless elder care system.

References

[1] J. Woo, S. C. Ho, J. Lau, S. G. Chan, and Y. K. Yuen, "Age-Associated Gait Changes in the Elderly: Pathological or Physiological?," *Neuroepidemiology*, vol. 14, no. 2, pp. 65–71, 1995.

[2] S. Kyeong, S. M. Kim, S. Jung, and D. H. Kim, "Gait pattern analysis and clinical subgroup identification: a retrospective observational study," *MEDICINE*, vol. 99, no. 15, 2020.

[3] E. Morel, S. Armand, F. Assal, and G. Allali, "Parkinsonian gait in aging: A feature of Alzheimer's pathology?," *Experimental Gerontology*, vol. 134, p. 110905, 2020.

[4] Kubicki and Alexandre, "Functional assessment in older adults: Should we use timed up and go or gait speed test?," *Neuroscience Letters*, vol. 577, no. 18, pp. 89–94, 2014.

[5] T. Wang, Z. Wang, D. Zhang, G. Tao, and L. Jing, "Recognizing Parkinsonian Gait Pattern by Exploiting Fine-Grained Movement Function Features," *Acm Transactions on Intelligent Systems & Technology*, vol. 8, no. 1, pp. 1–22, 2016.

[6] J. M. Viton, L. Bensoussan, M. Kerzoncuf, and A. Delarque, "Abnormal gait in patients with neurological pathologies," *Annals of Physical & Rehabilitation Medicine*, vol. 57, no. 4, pp. e428–e428, 2014.

[7] J. Fletcher, "What is abnormal gait?." https://www.medicalnewstoday.com/articles/320481. 2017.

[8] C. Werner, S. Schneider, R. Gassert, A. Curt, and L. Demkó, "Complementing Clinical Gait Assessments of Spinal Cord Injured Individuals using Wearable Movement Sensors," in *2020 42nd Annual International Conference of the IEEE Engineering in Medicine & Biology Society (EMBC)*, pp. 3142–3145, 2020.

[9] N. Takemura, Y. Makihara, D. Muramatsu, T. Echigo, and Y. Yagi, "On Input/Output Architectures for Convolutional Neural Network-Based Cross-View Gait Recognition," *IEEE Transactions on Circuits and Systems for Video Technology*, vol. 29, no. 9, pp. 2708–2719, 2017.

[10] H. Ma and W.-H. Liao, "Human Gait Modeling and Analysis Using a Semi-Markov Process With Ground Reaction Forces," *IEEE Transactions on Neural Systems and Rehabilitation Engineering*, vol. 25, no. 6, pp. 597–607, 2017.

[11] W. Xu, G. Lan, Q. Lin, S. Khalifa, M. Hassan, N. Bergmann, and W. Hu, "KEH-Gait: Using kinetic energy harvesting for gait-based user authentication systems," *IEEE Transactions on Mobile Computing*, vol. 18, no. 1, pp. 139–152, 2018.

[12] L. Zhang, C. Wang, M. Ma, and D. Zhang, "WiDIGR: Direction-Independent Gait Recognition System Using Commercial Wi-Fi Devices," *IEEE Internet of Things Journal*, vol. 7, no. 2, pp. 1178–1191, 2020.

[13] L. Zhang, C. Wang, and D. Zhang, "Wi-PIGR:Path Independent Gait Recognition with Commodity Wi-Fi," *IEEE Transactions on Mobile Computing*, vol. 21, no. 9, pp. 3414–3427, 2022.

[14] W. Wang, A. X. Liu, and M. Shahzad, "Gait Recognition Using Wifi Signals," in *Proceedings of the 2016 ACM International Joint Conference on Pervasive and Ubiquitous Computing*, pp. 363–373, 2016.

[15] Y. Zeng, P. H. Pathak, and P. Mohapatra, "WiWho: WiFi-Based Person Identification in Smart Spaces," in *2016 15th ACM/IEEE International Conference on Information Processing in Sensor Networks (IPSN)*, pp. 1–12, 2016.

[16] C. Lin, J. Hu, Y. Sun, F. Ma, L. Wang, and G. Wu, "WiAU: An Accurate Device-Free Authentication System with ResNet," in *2018 15th Annual IEEE International Conference on Sensing, Communication, and Networking (SECON)*, pp. 1–9, 2018.

[17] L. Zhang, Y. Zhang, B. Wang, X. Zheng, and L. Yang, "WiCrowd: Counting the Directional Crowd With a Single Wireless Link," *IEEE Internet of Things Journal*, vol. 8, no. 10, pp. 8644–8656, 2021.

[18] S. Liu, Y. Zhao, and B. Chen, "WiCount: A Deep Learning Approach for Crowd Counting Using WiFi Signals," in *2017 IEEE International Symposium on Parallel and Distributed Processing with Applications and 2017 IEEE International Conference on Ubiquitous Computing and Communications (ISPA/IUCC)*, pp. 967–974, 2017.

[19] C. Xu, B. Firner, R. S. Moore, Y. Zhang, and A. Ning, "SCPL: Indoor Device-Free Multi-Subject Counting and Localization Using Radio Signal Strength," in *Proceedings of the 12th International Conference on Information Processing in Sensor Networks*, pp. 79–90, 2013.

[20] F. Adib, Z. Kabelac, and D. Katabi, "Multi-Person Localization via RF Body Reflections," in *Networked Systems Design and Implementation*, pp. 279–292, 2015.

[21] Y. Zheng, Y. Zhang, K. Qian, G. Zhang, Y. Liu, C. Wu, and Z. Yang, "Zero-Effort Cross-Domain Gesture Recognition with Wi-Fi," in *Proceedings of the 17th Annual International Conference on Mobile Systems, Applications, and Services*, pp. 313–325, 2019.

[22] Z. Shi, J. A. Zhang, R. Xu, Q. Cheng, and A. Pearce, "Towards Environment-Independent Human Activity Recognition using Deep Learning and Enhanced CSI," in *GLOBECOM 2020 - 2020 IEEE Global Communications Conference*, pp. 1–6, 2020.

[23] I. Santamaria, "Handbook of blind source separation: Independent component analysis and applications (common, p. and jutten, ; 2010 [book review]," *IEEE Signal Processing Magazine*, vol. 30, no. 2, pp. 133–134, 2013.

[24] H. Chao, Y. He, J. Zhang, and J. Feng, "GaitSet: Regarding Gait as a Set for Cross-View Gait Recognition," vol. 33, no. 1, pp. 8126–8133, 2019.

[25] S. Pan, N. Wang, Y. Qian, I. Velibeyoglu, H. Y. Noh, and P. Zhang, "Indoor Person Identification through Footstep Induced Structural Vibration," in *Proceedings of the 16th International Workshop on Mobile Computing Systems and Applications*, pp. 81–86, 2015.

[26] M. Muaaz and R. Mayrhofer, "Smartphone-Based Gait Recognition: From Authentication to Imitation," *IEEE Transactions on Mobile Computing*, vol. 16, no. 11, pp. 3209–3221, 2017.

[27] L. Zhang, M. Liu, L. Lu, and L. Gong, "Wi-Run: Multi-Runner Step Estimation Using Commodity Wi-Fi," in *2018 15th Annual IEEE International Conference on Sensing, Communication, and Networking (SECON)*, pp. 1–9, 2018.

[28] X. Wang, C. Yang, and S. Mao, "PhaseBeat: Exploiting CSI Phase Data for Vital Sign Monitoring with Commodity WiFi Devices," in *2017 IEEE 37th International Conference on Distributed Computing Systems (ICDCS)*, pp. 1230–1239, 2017.

[29] B. Rao and K. Hari, "Performance Analysis Of Root-music," in *Twenty-Second Asilomar Conference on Signals, Systems and Computers*, pp. 578–582, 1988.

[30] Y. Yang, J. Cao, X. Liu, and K. Xing, "Multi-person Sleeping Respiration Monitoring with COTS WiFi Devices," in *2018 IEEE 15th International Conference on Mobile Ad Hoc and Sensor Systems (MASS)*, pp. 37–45, 2018.

[31] H. Wang, D. Zhang, J. Ma, Y. Wang, Y. Wang, D. Wu, T. Gu, and B. Xie, "Human Respiration Detection with Commodity WiFi Devices: Do User Location and Body Orientation Matter?," in *Proceedings of the 2016 ACM International Joint Conference on Pervasive and Ubiquitous Computing*, pp. 25–36, 2016.

[32] D. Zhang, H. Wang, and D. Wu, "Toward Centimeter-Scale Human Activity Sensing with Wi-Fi Signals," *Computer*, vol. 50, no. 1, pp. 48–57, 2017.

[33] R. H. Venkatnarayan, G. Page, and M. Shahzad, "Multi-User Gesture Recognition Using WiFi," in *Proceedings of the 16th Annual International Conference on Mobile Systems, Applications, and Services*, pp. 401–413, 2018.

[34] J. He and W. Yang, "IMar: Multi-User Continuous Action Recognition with WiFi Signals," *Proc. ACM Interact. Mob. Wearable Ubiquitous Technol.*, vol. 6, no. 3, pp. 1–27, 2022.

[35] S. Tan, L. Zhang, Z. Wang, and J. Yang, "MultiTrack: Multi-User Tracking and Activity Recognition Using Commodity WiFi," in *the 2019 CHI Conference*, 2019.

[36] F. Wang, F. Zhang, C. Wu, B. Wang, and K. J. R. Liu, "Respiration Tracking for People Counting and Recognition," *IEEE Internet of Things Journal*, vol. 7, no. 6, pp. 5233–5245, 2020.

[37] C. Feng, S. Arshad, S. Zhou, D. Cao, and Y. Liu, "Wi-Multi: A Three-Phase System for Multiple Human Activity Recognition With Commercial WiFi Devices," *IEEE Internet of Things Journal*, vol. 6, no. 4, pp. 7293–7304, 2019.
[38] A. Hyvarinen, J. Karhunen, and E. Oja, "Independent Component Analysis," *Studies in Informatics and Control*, vol. 11, no. 2, pp. 205–207, 2002.
[39] X. Li, D. Zhang, Q. Lv, J. Xiong, S. Li, Y. Zhang, and H. Mei, "IndoTrack: Device-Free Indoor Human Tracking with Commodity Wi-Fi," *Proceedings of the ACM on Interactive, Mobile, Wearable and Ubiquitous Technologies*, vol. 1, no. 3, pp. 1–22, Sep 2017.
[40] M. Kotaru, K. Joshi, D. Bharadia, and S. Katti, "SpotFi: Decimeter Level Localization Using WiFi," in *Proceedings of the 2015 ACM Conference on Special Interest Group on Data Communication*, pp. 269–282, 2015.
[41] X. Li, S. Li, D. Zhang, J. Xiong, Y. Wang, and H. Mei, "Dynamic-MUSIC: Accurate Device-Free Indoor Localization," in *Proceedings of the 2016 ACM international joint conference on pervasive and ubiquitous computing*, pp. 196–207, 2016.
[42] V. Zarzoso and P. Comon, "Robust Independent Component Analysis by Iterative Maximization of the Kurtosis Contrast With Algebraic Optimal Step Size," *IEEE Transactions on Neural Networks*, vol. 21, no. 2, pp. 248–261, 2010.
[43] Y. Zeng, D. Wu, J. Xiong, E. Yi, R. Gao, and D. Zhang, "FarSense: Pushing the Range Limit of WiFi-Based Respiration Sensing with CSI Ratio of Two Antennas," *Proceedings of the ACM on Interactive, Mobile, Wearable and Ubiquitous Technologies*, vol. 3, no. 3, pp. 1–26, 2019.
[44] J.-Y. Zhu, T. Park, P. Isola, and A. A. Efros, "Unpaired Image-to-Image Translation Using Cycle-Consistent Adversarial Networks," in *2017 IEEE International Conference on Computer Vision (ICCV)*, pp. 2242–2251, 2017.
[45] T. D. Bel, J. M. Bokhorst, J. Laak, and G. Litjens, "Residual CycleGAN for robust domain transformation of histopathological tissue slides," *Medical Image Analysis*, vol. 70, no. 2, p. 102004, 2021.
[46] Z. Zhao, X. Chen, B. Li, Y. Wang, and Q. Liu, "Range-Doppler Spectrograms-Based Clutter Suppression of HF Passive Bistatic Radar by D-CycleGAN," *IEEE Sensors Journal*, vol. 21, no. 22, pp. 26006–26013, 2021.
[47] C. Li, H. Liu, C. Chen, Y. Pu, L. Chen, R. Henao, and L. Carin, "ALICE: Towards Understanding Adversarial Learning for Joint Distribution Matching," in *Advances in Neural Information Processing Systems*, pp. 5501–5509, 2017.
[48] J. Johnson, A. Alahi, and L. Fei-Fei, "Perceptual Losses for Real-Time Style Transfer and Super-Resolution," in *Computer Vision – ECCV 2016*, pp. 694–711, 2016.
[49] D. Ulyanov, A. Vedaldi, and V. Lempitsky, "Instance Normalization: The Missing Ingredient for Fast Stylization," 2016.
[50] P. Isola, J.-Y. Zhu, T. Zhou, and A. A. Efros, "Image-to-Image Translation with Conditional Adversarial Networks," in *2017 IEEE Conference on Computer Vision and Pattern Recognition (CVPR)*, pp. 5967–5976, 2017.
[51] D. Halperin, W. Hu, A. Sheth, and D. Wetherall, "Tool Release: Gathering 802.11n Traces with Channel State Information," *SIGCOMM Comput. Commun. Rev.*, vol. 41, no. 1, p. 53, 2011.
[52] D. Kingma and J. Ba, "Adam: A method for stochastic optimization," *Computer Science*, 2014.
[53] F. Adib, H. Mao, Z. Kabelac, D. Katabi, and R. C. Miller, "Smart Homes that Monitor Breathing and Heart Rate," in *Proceedings of the 33rd Annual ACM Conference on Human Factors in Computing Systems*, p. 837–846, 2015.
[54] X. Wang, K. Niu, J. Xiong, B. Qian, Z. Yao, T. Lou, and D. Zhang, "Placement Matters: Understanding the Effects of Device Placement for WiFi Sensing," *Proceedings of the ACM on Interactive, Mobile, Wearable and Ubiquitous Technologies*, vol. 6, no. 1, pp. 1–25, 2022.
[55] Bohannon and W. Richard, "Comfortable and maximum walking speed of adults aged 20-79 years: Reference values and determinants.," *Age & Ageing*, vol. 26, no. 1, pp. 15–19, 1997.
[56] S. L. Fritz and M. Lusardi, "Walking speed: the sixth vital sign," *Journal of Geriatric Physical Therapy*, vol. 32, no. 2, p. 46–49, 2009.
[57] X. Guo, J. Liu, C. Shi, H. Liu, Y. Chen, and M. C. Chuah, "Device-free personalized fitness assistant using wifi," *Proceedings of the Acm on Interactive Mobile Wearable & Ubiquitous Technologies*, vol. 2, no. 4, pp. 1–23, 2018.
[58] V. Sánchez A, "Frontiers of research in BSS/ICA," *Neurocomputing*, vol. 49, no. 1-4, pp. 7–23, 2002.
[59] Y. Yang, J. Cao, X. Liu, and X. Liu, "Wi-Count: Passing People Counting with COTS WiFi Devices," in *2018 27th International Conference on Computer Communication and Networks (ICCCN)*, pp. 1–9, 2018.
[60] S. Di Domenico, M. De Sanctis, E. Cianca, and G. Bianchi, "A Trained-Once Crowd Counting Method Using Differential WiFi Channel State Information," in *Proceedings of the 3rd International on Workshop on Physical Analytics*, pp. 37–42, 2016.
[61] Y. K. Cheng and R. Y. Chang, "Device-Free Indoor People Counting Using Wi-Fi Channel State Information for Internet of Things," in *GLOBECOM 2017 - 2017 IEEE Global Communications Conference*, pp. 1–6, 2017.

Lei Zhang received her Ph.D. degree in Computer Science from Auburn University (Auburn, AL, USA) in 2008, and worked as an assistant professor from 2008-2011 in the Computer Science Dept. at Frostburg State University (Frostburg, MD, USA); She is now an associate professor in College of Intelligence and Computing at Tianjin University (Tianjin, P.R. China). Her research interests include mobile computing and data mining. She is a member of the ACM and IEEE.

Yazhou Ma received the B.E. degree from Shanxi Agricultural University, Shanxi, China, in 2021. He is currently pursuing master degree at Tianjin University, Tianjin, China. His research interests include wireless sensing and data mining.

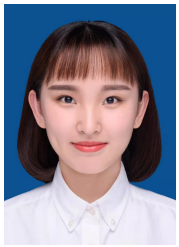

Xiaojie Fan received the B.E. degree from Tiangong University, Tianjin, China, in 2019, and M.Eng. degree from Tianjin University, Tianjin, China, in 2022. Her research interests include wireless communication and data mining.

Xiaochen Fan is a PostDoc Researcher at the Institute for Electronics and Information Technology in Tianjin and the Department of Electronic Engineering, Tsinghua University. He received the B.E. degree from the Beijing Institute of Technology in 2013 and the Ph.D. degree from the University of Technology Sydney in 2021, respectively. His research interests include urban science, wireless networks, deep learning, and spatio-temporal data mining.

Yonggang Zhang received the Ph.D. degree from the College of Computer Science and Technology, Jilin University, Changchun, China, in 2005. He was a Post-Doctoral Fellow with the School of Mathematics, Jilin University, Changchun, China, from 2007 to 2009. He is currently a Professor with the College of Computer Science and Technology, Jilin University, Changchun, China. His current research interests include constraint programming and artificial intelligence.

Zhenxiang Chen received the B.S. and M.S. degrees from the University of Jinan, Jinan, China, in 2001 and 2004, respectively, the Ph.D. degree from the School of Computer Science and Technology, Shandong University, Jinan, in 2008. He is currently a Professor with the School of Information Science and Engineering, University of Jinan. His research interests include network behavior analysis, mobile security and privacy, and intelligent information processing. In this area, he has authored over 130 papers in professional international peer-reviewed journals and conferences, such as IEEE Transactions on Information Forensics and Security (TIFS), IEEE Transactions on Knowledge and Data Engineering (TKDE), and IEEE/ACM International Symposium on Quality of Service (IWQOS).

Xianyi Chen received his PhD in Computer Science and Technology from Hunan University, China, in 2014. He is a visiting fellow of the Mathematics and Computer Science, The University of North Carolina at Pembroke, USA, in 2018-2019. Currently, he is a vice professor in the School of Computer and Software, Nanjing University of Information Science & Technology, China. His research interests include big data base information hiding, digital watermarking and AI security.

Daqing Zhang is a Professor with Peking University, China and IP Paris, France. His research interests include ubiquitous computing, context-aware computing, big data analytics and Intelligent IoT. He is the winner of the Ten Years CoMoRea Impact Paper Award at IEEE PerCom 2013 and Ten Years Most Influential Paper Award at IEEE UIC 2019, the Best Paper Award Runner-up at ACM MobiCom 2022, the Distinguished Paper Award of IMWUT (Ubicomp 2021), Honorable Mention Award at ACM UbiComp 2015 and 2016, etc.. He served as the general or program chair for more than a dozen of international conferences, and in the editorial board of IEEE Pervasive Computing and Proceeding of ACM IMWUT. Daqing Zhang is a Fellow of IEEE and Member of Academy of Europe.